

# Tracking of User Position and Orientation by Stereo Measurement of Infrared Markers and Orientation Sensing

Masaki Maeda<sup>†</sup>

Takefumi Ogawa<sup>† ‡</sup>

Kisyoshi Kiyokawa<sup>† ‡</sup>

Haruo Takemura<sup>† ‡</sup>

<sup>†</sup> Graduate school of Information Science and Technology, Osaka University

<sup>‡</sup> Infomedia Education Division, Cybermedia Center, Osaka University

*masaki-m@lab.imecmc.osaka-u.ac.jp*

*{ogawa, kiyo, takemura}@imecmc.osaka-u.ac.jp*

## Abstract

A real-time three-dimensional position and orientation tracking system is proposed for use with wearable augmented-reality systems. The system combines infrared markers with a head-mounted stereo camera to detect the user's position, and an orientation sensor to measure the orientation of the user's head. An extended Kalman filter is employed to reduce triangulation and orientation error by integrating the signals acquired by multiple sensors. The system is evaluated through a series of experiments, and a navigation system implemented using the proposed scheme is present. The accuracy of the system is shown to be sufficient to allow annotations and virtual objects to be overlaid on real scenes via a head-mounted display without confusion.

## 1. Introduction

Augmented reality (AR) has made it possible to provide users with intuitive and efficient information services [1]. An example is sightseeing, where a user can receive detailed information of various sightseeing locations. Using AR techniques, such information can be presented on a display device such as a head-mounted display (HMD), overlaying virtual objects on the real environment. In order to provide a user with appropriate information according to the user's location and orientation, it is important to establish a real-time measurement technology to monitor these parameters in three-dimensional space [14]. Many devices have been developed to acquire such three-dimensional position or orientation information, including the global positioning system (GPS) [3,10], magnetic position sensors, ultrasonic distance sensors

[3], and optical sensor using synchronous light-emitting and photo diodes [13]. However, these devices are unsuitable for position detection in a large indoor environment such as a building due to high cost or poor measurement accuracy. ARTToolkit [5], a vision-based marker tracking toolkit, is a popular and inexpensive means of user location. Although there have also been many other vision-based studies [4,9], most have found it difficult to identify and detect distant markers in a dark environment. The use of a pedometer [1,7,12] or natural feature tracking [6,11] has also been investigated as a means of expanding the working area by measuring the relative movement distance. However, pedometers are prone to cumulative error, and natural feature tracking is somewhat unstable in large working areas. Hallaway et al. proposed an inexpensive, coarse tracking system using infrared beacons in an indoor environment [2]. However, the proposed system only determined the two-dimensional position of the user's head.

In this paper, a hybrid tracking technique is proposed in which a stereo-camera and an orientation sensor are combined to estimate the three-dimensional position and orientation of a user's head. An AR navigation system based on the proposed location method is also presented. In the proposed system, most markers can be casually placed without the need for calibration, as unknown markers in the workspace are automatically mapped. The proposed method is robust with respect to lighting conditions, also working in complete darkness, and is less obtrusive in terms of aesthetics compared with many marker-based approaches.

The remainder of the paper is organized as follows. Section 2 provides an overview of the hybrid tracking technique, and section 3 describes the details of the

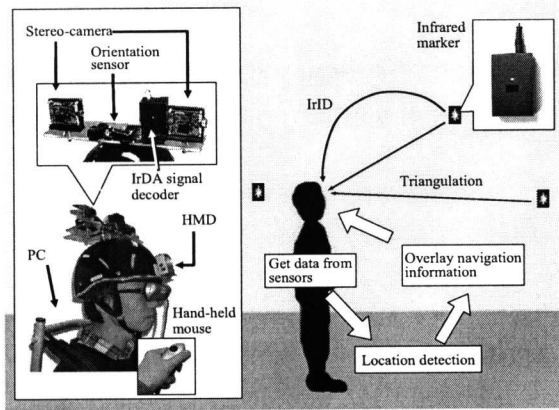


**Figure 1. Overview of proposed tracking system**

method. Section 4 presents the results of experiments and evaluates the effectiveness of the method, and section 5 describes the AR navigation system as a practical implementation. Finally, the paper is concluded in section 6, and possible future work is outlined.

## 2. Overview of hybrid tracking system

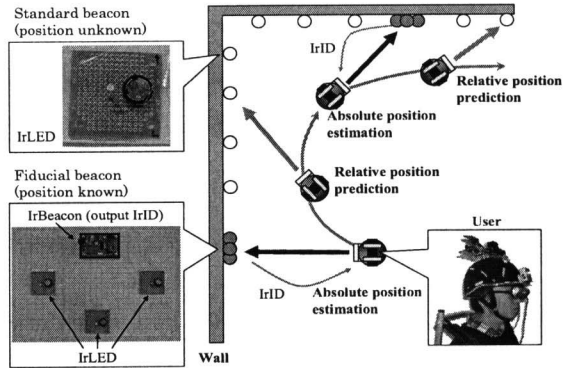
### 2.1. System configuration

Figure 1 presents an overview of the proposed hybrid tracking method. The user wears a helmet equipped with a stereo camera (Dragonfly, Point Gray Research) and infrared (IR) filter, an orientation sensor (InterTrax<sup>2</sup>, InterSense) composed of three gyro sensors, three geomagnetic sensors and two inertial sensors, and an infrared data association (IrDA) signal decoder. These devices are connected to a laptop computer in a backpack. The user also wears an HMD (Eye-Trek, Olympus).

Infrared light-emitting diode (LED) markers are placed sparsely throughout the working area. Some of the markers emit unique identifiers using an IrDA signal (called IrBeacons), while the others emit generic signals (called IrLEDs). The system detects these infrared markers from the IR-filtered camera images and calculates the position and orientation of the user's head relative to the markers by stereo matching. Virtual objects such as annotations can then be overlaid onto the real environment seen through the HMD.

### 2.2. Arrangement of infrared markers

In most existing marker-based approaches, the world coordinates of each marker need to be given in



**Figure 2. Absolute position estimation and relative position prediction**

advance in order to estimate the user's position and orientation. This means that during construction of the system, the world coordinates of all markers need to be measured and registered in a database, making it very difficult to expand the workspace. In contrast, the proposed method requires only a few sets of infrared markers to be measured in advance. These infrared markers are called fiducial beacons. Once the system initializes the user's position and orientation using a fiducial beacon, it can repeatedly calculate relative motion using a single infrared marker with unknown world coordinates (called standard beacons). Figure 2 provides an overview of absolute position estimation and relative position prediction using this approach, along with photographs of the standard and fiducial beacons. The standard beacon is composed of an IrLED, and can be placed arbitrarily in the workspace. The fiducial beacon is composed of an IrBeacon and three IrLEDs, and its world coordinates are known. The system can identify the IrBeacon of a fiducial beacon by decoding its identifier (IrID) through the IrDA signal decoder.

### 2.3. Feature summary

The main features of the proposed tracking scheme are summarized below.

**Facilitates workspace expansion:** Most markers can be casually placed without the need for calibration, as unknown markers in the workspace are automatically mapped and registered in the database.

**Robustness with respect to lighting conditions:** The system functions under a variety of lighting conditions, including in complete darkness, due to the use of infrared markers.

**Minimally intrusive:** As the infrared light is invisible to humans and only the tip of an infrared LED needs to

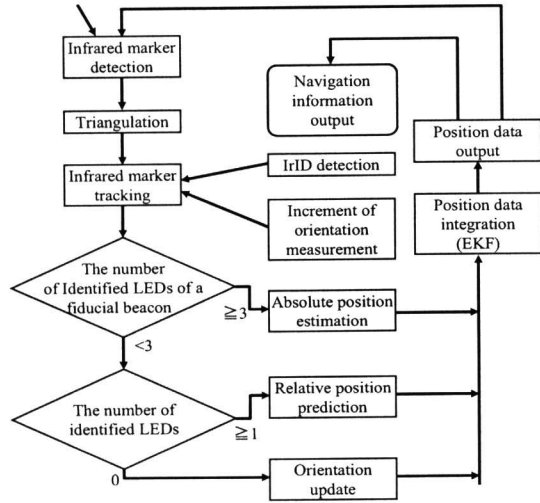


**Figure 3. Flow diagram of tracking system**

be seen (circuit boards can be hidden), the markers are relatively less obtrusive in terms of aesthetics compared with many marker-based approaches.

**IrDA communication:** An IrBeacon can be used for data communication in location-based applications [8].

### 3. Measuring the position and orientation of a user's head

#### 3.1. Flow of hybrid tracking

Figure 3 shows a flow diagram of the proposed hybrid tracking scheme. The tracking algorithm proceeds as follows:

1. If an infrared marker is detected, the system calculates the relative distance from the marker to the center of the stereo camera pair (Section 3.2).
2. If the IrDA signal decoder receives an IrID, the system identifies the infrared marker using the IrID and tracks it.
3. If three or more LEDs of a fiducial beacon are detected, the system calculates the user's absolute position using absolute position estimation method (Section 3.3).
4. If one or two LEDs are detected, the system predicts the user's current position using relative motion and user's last position (Section 3.4).
5. If no LEDs are detected, the system updates only the user's orientation.
6. The system reduces position and orientation error by employing an extended Kalman filter (Section 3.5).

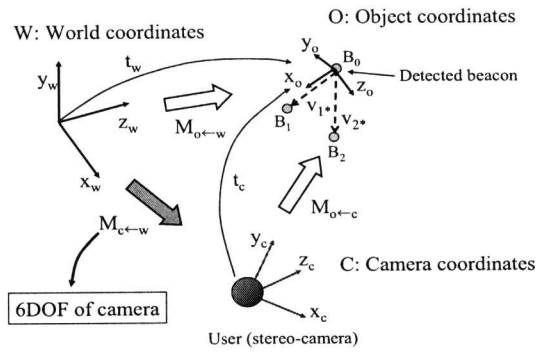


**Figure 4. Absolute position estimation**

#### 3.2. Beacon detection and identification

The system detects IR light captured as a pair of stereo images. An IR filter is attached to each camera lens to facilitate the detection of infrared marker areas. If two matching areas are found in the left and right images, the camera coordinates of the infrared marker are measured by triangulation. If the detected infrared marker is an IrBeacon, its IrID is also detected by the IrDA signal decoder, which is mounted adjacent to the cameras. The system then retrieves the information for the fiducial beacon from the database using the IrID. The three IrLEDs of the fiducial beacon can be identified immediately by the geometric constraints of their layout.

The system also dynamically defines an identifier for unregistered infrared markers. Using the user's orientation, the system predicts the screen coordinates of the infrared markers in the next frame based on the coordinates of the present frame. The infrared markers can then be tracked by matching the predicted and detected screen coordinates.

#### 3.3. Absolute position estimation

The system requires at least three known markers to calculate the 6 degree-of-freedom (6DOF) location of the user from the stereo images. Figure 4 gives an overview of absolute position estimation.  $B_0$ ,  $B_1$ , and  $B_2$  denote the three detected beacons, and  $V_{1w}$  and  $V_{2w}$  are the vectors from  $B_0$  to  $B_1$  and from  $B_0$  to  $B_2$  in world coordinates.  $V_{1c}$  and  $V_{2c}$  are vectors from  $B_0$  to  $B_1$  and from  $B_0$  to  $B_2$  in camera coordinates. An asterisk "\*" is used to denote "w" (world) or "c" (camera) coordinates. The object coordinates are defined such that the  $x$ ,  $y$ , and  $z$  axes are parallel to  $V_{1*}$ ,  $V_{1*} \times V_{2*}$ , and  $(V_{1*} \times V_{2*}) \times V_{1*}$ , respectively. Using these vectors, the transformation matrix from world

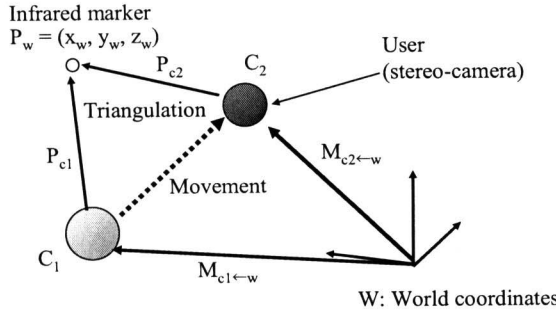


**Figure 5. Relative position prediction**

coordinates or camera coordinates to object coordinates  $M_{o \leftarrow *}$  is expressed as follows.

$$M_{o \leftarrow *} = \begin{pmatrix} e_{x*} & e_{y*} & e_{z*} & t_* \\ 0 & 0 & 0 & 1 \end{pmatrix} \quad (1)$$

where  $e_{x*}$ ,  $e_{y*}$ , and  $e_{z*}$  are base vectors of the object coordinates and  $t_*$  is the translation from world or camera coordinates to object coordinates. Therefore, the matrix  $M_{c \leftarrow w}$  from world coordinates to camera coordinates is expressed by

$$M_{c \leftarrow w} = (M_{o \leftarrow c})^{-1} M_{o \leftarrow w} \quad (2)$$

### 3.4. Relative position prediction

If only one or two infrared markers of a fiducial beacon are detected, the system cannot calculate all of the user's 6DOF information. In this case, the system reduces the number of unknown parameters by updating the user's orientation using the orientation sensor, and then calculating the user's position by stereo triangulation.

Assuming that the position and orientation of the camera in the world coordinates are known, it is in fact possible to calculate the world coordinates of an unknown infrared marker (standard beacon) in view. If the camera moves or rotates during a frame, the position of the camera in the world coordinates can be calculated from the angular displacement and relative position of the tracked infrared marker to the camera by triangulation. The system continues to track the infrared marker once it has been registered in the database, and then if an unknown standard beacon is detected in a frame, the system registers that beacon in the database and tracks it in the same way. Thus, even if there is only one known infrared marker in a camera frame, it is still possible to predict the position and orientation of the camera continuously. Figure 5 presents an overview of relative position prediction.

Let  $M_{c1 \leftarrow w}$  and  $P_{c1}$  denote the transformation matrix from world to camera coordinates, and the position of

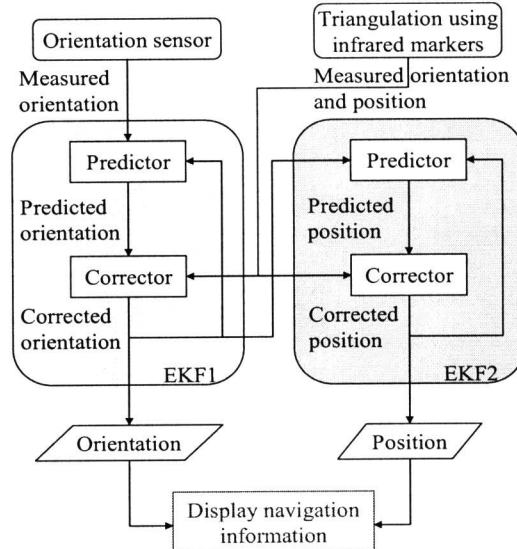


**Figure 6. Integration of data using an Extended Kalman Filter**

the marker in the previous frame in camera coordinates. The position  $P_w = (x_w, y_w, z_w)$  of the marker in the next frame is then expressed by

$$P_w = (M_{c1 \leftarrow w})^{-1} P_{c1} \quad (3)$$

Therefore, the position of the infrared marker in the next frame in camera coordinates is expressed by the following equation in terms of  $P_w$  and  $M_{c2 \leftarrow w}$ .

$$\begin{aligned} P_{c2} &= M_{c2 \leftarrow w} P_w \\ &= R_{c2 \leftarrow w} T_{c2 \leftarrow w} P_w \end{aligned} \quad (4)$$

where  $R_{c2 \leftarrow w}$  and  $T_{c2 \leftarrow w}$  express the rotation and translation components of  $M_{c2 \leftarrow w}$ , respectively. Here,  $R_{c2 \leftarrow w}$  is given by the orientation sensor. Thus, the unknown parameter is a moving vector  $t = (t_x, t_y, t_z)$  in  $T_{c2 \leftarrow w}$ , where  $t_x$ ,  $t_y$ , and  $t_z$  are the moving distances along the  $x$ ,  $y$ , and  $z$  axes in world coordinates. Then, letting

$$(R_{c2 \leftarrow w})^{-1} P_{c2} = (r_{cx} \ r_{cy} \ r_{cz} \ 1)^T \quad (5)$$

gives

$$\begin{pmatrix} r_{cx} \\ r_{cy} \\ r_{cz} \\ 1 \end{pmatrix} = \begin{pmatrix} x_w + t_x \\ y_w + t_y \\ z_w + t_z \\ 1 \end{pmatrix} \quad (6)$$

By solving this equation,  $(t_x, t_y, t_z)$  can be calculated. As the triangulation error affects the prediction accuracy, if two or more known infrared markers are detected in the image, the closest marker to the camera is used.

### 3.5. Position and direction correction by EKF

The predicted position data include jitter due to triangulation error, and the orientation data include error due to drift of the gyro sensor and geomagnetic distortion. The error and jitter of these data are reduced in the proposed scheme by integrating the position data and the orientation data using an extended Kalman filter (EKF). Figure 6 shows the flow diagram for the EKF used in this scheme.

The EKF for orientation prediction corrects orientation data using two sets of orientation data, one derived from the orientation sensor, and another derived from the infrared markers. The state vector is represented by a rotation quaternion. The covariance parameters  $Q$  and  $R$  for process and measurement noise are determined heuristically. Both  $Q$  and  $R$  change dynamically based on the active procedure for position and orientation detection. For example,  $R$  approaches zero for relative position prediction, and increases for absolute position estimation. The EKF for position prediction corrects position data using orientation data from the first EKF and position data calculated using the IR markers. The state vector in this case is a six-tuple  $(x, y, z, x', y', z')$  composed of user's position and velocity. By recording velocity data, the system can estimate the user's movement distance even when no infrared marker is found.

When three or more infrared markers of fiducial beacons are detected, it is possible to reduce both triangulation error and drift of the orientation sensor. However, when less than three infrared markers are detected, orientation data is measured only by the orientation sensor. In this case, it is impossible to reduce orientation error.

## 4. Experiments

Three experiments were conducted to evaluate the performance of the proposed tracking scheme. The configuration of each of the experiments is presented below and the results discussed.

### 4.1. Experiment 1: Measurement accuracy while standing

#### (1) Experimental setting

In this experiment, the position of a subject was calculated while standing at distances of 1, 1.5, and 2 m from a fiducial beacon mounted on a wall to examine the effects of distance from the fiducial beacon to the camera with and without EKF. Figure 7(a) shows the setting of the experiment.

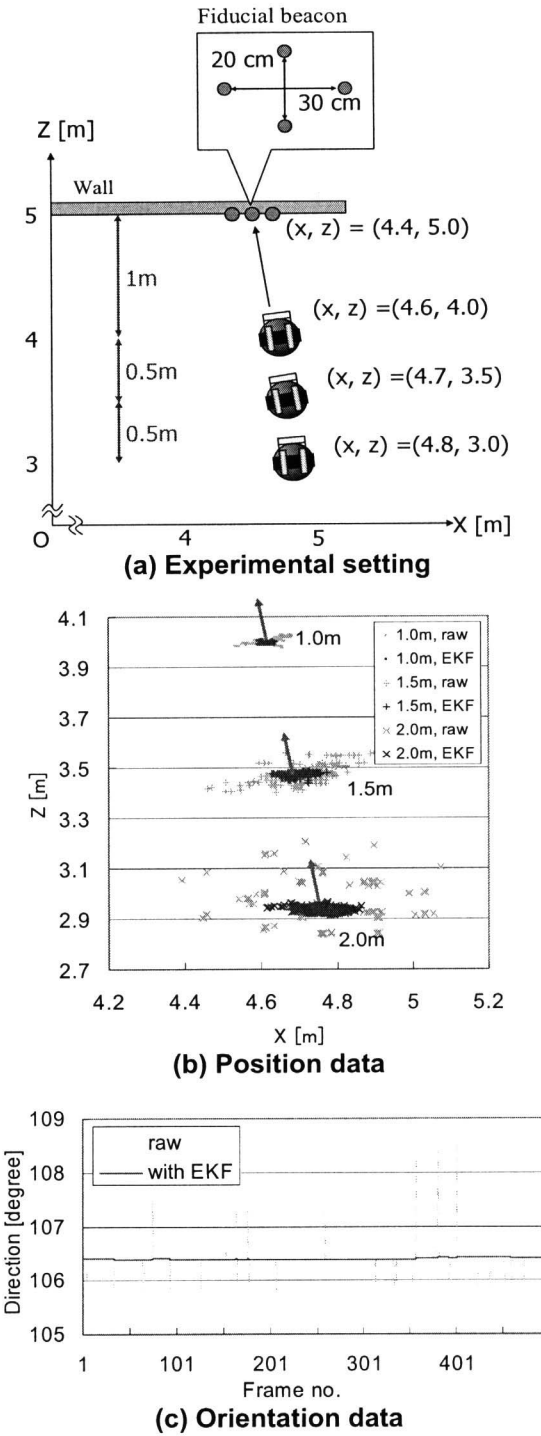


**Figure 7. Setting and results of experiment 1**

#### (2) Results and discussion

Figures 7(b) and (c) show the results of measurement, where Figure 7(b) shows the distribution

of measured position data in plan view. The arrows in the graph represent the orientation of the camera at each standing point. The triangulation error increases with distance between the camera and the infrared marker, resulting in degraded measurement accuracy. Without EKF, jitter on the  $x$  axis is less than about 8 cm at a distance of 1 m, and 35 cm at a distance of 2 m from the fiducial beacon. With EKF, the jitter is reduced to less than 2.5, 7, and 12 cm at distances of 1, 1.5, and 2 m from the fiducial beacon. These results confirm that EKF reduces jitter by approximately 70%.

Figure 7(c) shows the measured orientation data with the subject standing 1.5 m from the fiducial beacon. Without EKF, jitter is less than  $3^\circ$ , decreasing to less than  $0.3^\circ$  with EKF. Thus, it was confirmed that EKF improves the measurement accuracy by integrating position and orientation data.

#### 4.2. Experiment 2: Registration accuracy

##### (1) Experimental setting

The registration error was examined by evaluating the difference between the observed and target positions of virtual objects on the screen. The HMD had a horizontal viewing angle of about  $30^\circ$ , with resolution of  $640 \times 480$  pixels. The camera was placed 1.5 m from the fiducial beacon, and the virtual objects were prepared so as to appear at the center of four infrared markers, as shown in Figure 8(a).

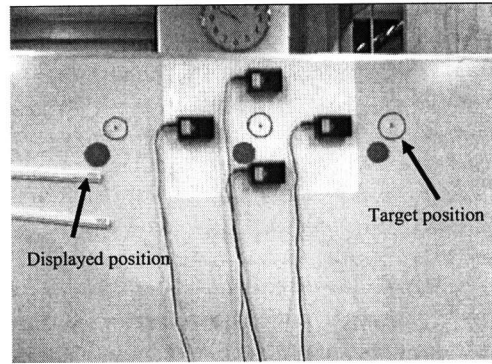
##### (2) Results and discussion

Figure 8(b) shows the screen coordinates of the objects displayed on the HMD, with origin at the target position. Table 1 shows the registration error for the virtual objects. It is apparent that the displayed position of a virtual object is shifted to the lower left from the target position by about 40 pixels. This is mainly due to calibration error between the stereo camera pair and the camera for video see-through observation, and also due to triangulation error caused by lens distortion. Existing accurate camera calibration methods are expected to reduce this registration error significantly [9], although this error (less than  $3^\circ$  visual angle) is sufficiently small to allow text to be read without confusion.

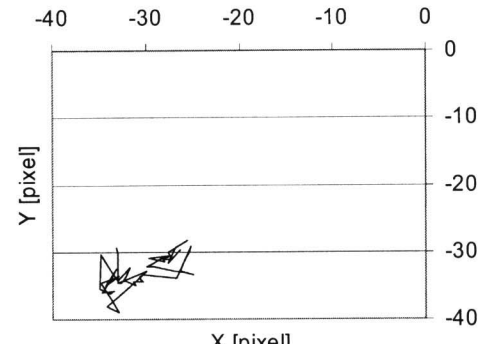
#### 4.3. Experiment 3: Measurement accuracy while walking

##### (1) Experimental setting

Another experiment was performed to evaluate the accuracy of the tracking scheme when the subject is walking in a corridor. Figure 9(a) shows the



**(a) Target and displayed positions of virtual objects**



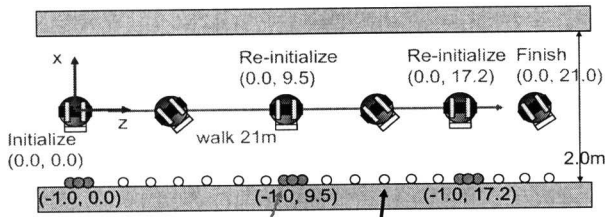
**(b) Displacement on the screen**

**Figure 8. Setting and results of experiment 2**

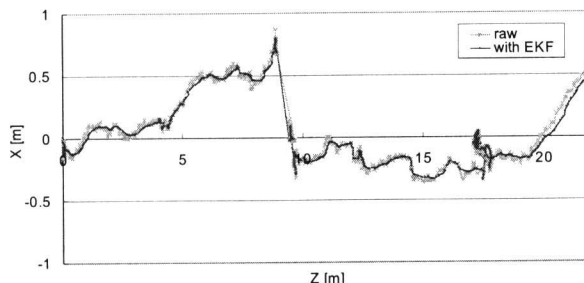
experimental setting. The subjects initialized their position by looking at the fiducial beacon at the starting point  $((X, Z) = (0.0, 0.0))$ , and then each subject walked along the centerline of the corridor to the target point  $((X, Z) = (0.0, 21.0))$  at a speed of 1 m/s. A total of 14 standard beacons were placed on the wall at intervals of about 1.5 m. The system predicts the distance moved by the user using the relative position prediction method. Fiducial beacons were also placed at the start,  $(X, Z) = (0.0, 9.5)$  and  $(X, Z) = (0.0, 17.2)$ . Consequently, it was possible to reset the error by absolute position estimation at the fiducial beacons.

**Table 1. Registration error in experiment 2**

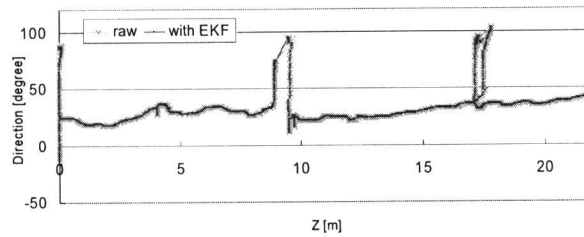
Error [pixel]	Minimum	Maximum	Average	Variance
X [pixel]	-34.986	-24.919	-30.703	9.480
Y [pixel]	-38.901	-28.248	-32.974	4.953
Distance	38.137	51.167	45.090	11.301



**(a) Experimental setting**



**(b) Position data**



**(c) Orientation data**

**Figure 9. Setting and results of experiment 3**

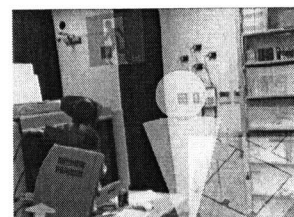
## (2) Results and discussion

Figures 9(b) and (c) show the transition of horizontal position and orientation (yaw) of the subject. When the subject walked from the start point to  $(X, Z) = (0.0, 9.5)$ , the measured subject position was  $(X, Z) = (0.97, 8.95)$  due to orientation error of about  $6^\circ$  from the start point. However, the system subsequently corrected the subject's position and orientation (yaw) to  $(X, Z) = (0.03, 9.46)$  and about  $92^\circ$  by absolute position estimation using the second fiducial beacon at  $(X, Z) = (-1.0, 9.5)$ . As the subject walked from  $(X, Z) = (0.0, 9.5)$  to  $(X, Z) = (0.0, 17.2)$ , the error along the  $x$  axis remained very small because the orientation error was minimized. However, the measured distance moved by the subject was longer than the actual distance due to the accumulation of position error caused by errors in triangulation. As a result, when the subject reached  $(X, Z) = (0.0, 17.2)$ , the position measured by the system was  $(X, Z) = (-0.18, 17.8)$ . The

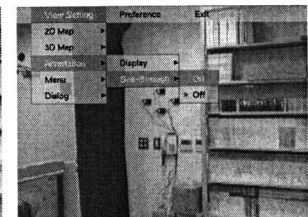


**(a) Annotations**

**(b) 3D floor map**



**(c) Avatar**



**(d) 2D menu**

**Figure 10. Overview of AR-Navi system**

system corrected the position and orientation (yaw) of the subject to  $(X, Z) = (-0.01, 17.19)$  and about  $88^\circ$  by absolute position estimation using the third fiducial beacon at  $(X, Z) = (-1.0, 17.2)$ . The position of the subject measured by the system when the user reached the target was  $(X, Z) = (0.48, 21.8)$ . Thus, the system maintained a position error of less than 1 m while the subject moved a distance of 10 m.

## 5. AR-Navi

### 5.1. Overview of AR-Navi

Our group has developed a navigation system (AR-Navi) that provides AR information via a wearable AR system. Figure 10 gives an overview of AR-Navi. The AR-Navi system navigates a user by overlaying navigation information onto the real scene based on the user's location using a see-through HMD. The system shows a map of the user's current environment after successful acquisition of the user's position, and virtual objects are then displayed over the real image as shown in Figure 10(a).

With a hand-held input device, the user can set a destination on the three-dimensional map, which appears on the screen on-demand. The system finds the shortest path from the user's current position to the destination, and then displays the navigation route on the map, as shown in Figure 10(b). The shortest path is updated in real-time in response to the user's movement. After the user has finished setting a destination, an arrow indicating the direction to the destination is overlaid on the real scene and the map disappears. The system overlays an avatar at the

destination, as shown in Figure 10(c). The user can configure various properties and functions via a menu as shown in Figure 10(d). This allows the user to adjust settings such as whether to display a two-dimensional map or annotations, and adjusting the display size of the map to be adjusted.

## 5.2. Display of navigation information

In AR-Navi, the entire workspace is divided into multiple areas using boundaries such as walls, and the system maintains an area database as a weighted graph with nodes to represent each area. When the user's position is detected, the system searches for two areas, the current position and the destination, and calculates the shortest path between the areas using Dijkstra's algorithm. The annotation information defined in current area and navigation information to the destination is then shown to the user.

## 6. Conclusions and future work

This paper described a hybrid tracking technique that combines a stereo-camera with an orientation sensor to locate and orientate the user's head in three-dimensional space. A navigation system based on the proposed method was also presented. The location accuracy of the system was evaluated through a series of experiments that showed that the error for a stationary subject is less than about 10 cm, while that for a moving subject is within 10% of the movement distance. Thus, it was confirmed that this system is sufficiently accurate to display navigational information via a wearable AR system.

The advantages of the proposed tracking system over existing techniques include the ease of expanding the workspace, the robustness of tracking under adverse lighting conditions, its minimally intrusive appearance, and its IrDA communication capability.

As part of future work, the authors intend to explore the potential of this tracking technique, improve the maintenance of navigational information, and develop multi-user information sharing via a network.

## Acknowledgments

This research was supported in part by the Core Research for Evolutional Science and Technology (CREST) Program "Advanced Media Technology for Everyday Living" of the Japan Science and Technology Corporation (JST).

## References

- [1] R. Azuma "A Survey of Augmented Reality," *Presence: Teleoperators and Virtual Environments*, Vol. 6, No. 4, pp. 355-385, 1997.
- [2] D. Hallaway, T. Höllerer and S. Feiner, "Coarse, Inexpensive, Infrared Tracking for Wearable Computing," *Proc. of the 7<sup>th</sup> IEEE International Symposium on Wearable Computers (ISWC03)*, pp. 69-78, Oct. 2003.
- [3] T. Höllerer, S. Feiner, T. Terauchi, G. Rashid and D. Hallaway, "Exploring MARS: Developing Indoor and Outdoor User Interfaces to a Mobile Augmented Reality System," *Computers and Graphics*, Vol. 23, No. 6, pp. 779-785, Dec. 1999.
- [4] M. Kalkusch, T. Lidy, M. Knapp, G. Reitmayr, H. Kaufmann and D. Schmalstieg, "Structured Visual Markers for Indoor Pathfinding," *Proc. of the 1<sup>st</sup> IEEE International Augmented Reality Toolkit Workshop (ART02)*, Sep. 2002.
- [5] H. Kato, M. Billinghurst, I. Poupyrev, K. Imamoto and K. Tachibana, "Virtual Object Manipulation on a Table-Top AR Environment," *Proc. of ISAR 2000*, pp. 111-119, Oct. 2000.
- [6] G. Klein and T. Drummond, "Robust Visual Tracking for Non-Instrumented Augmented Reality," *Proc. of the 2<sup>nd</sup> IEEE and ACM International Symposium on Mixed and Augmented Reality (ISMAR03)*, pp. 113-122, Oct. 2003.
- [7] M. Kourogi and T. Kurata, "Personal Positioning based on Walking Locomotion Analysis with Self-Contained Sensors and a Wearable Camera," *Proc. of the 2<sup>nd</sup> IEEE and ACM International Symposium on Mixed and Augmented Reality (ISMAR03)*, pp. 103-112, Oct. 2003.
- [8] G. Q. Maguire, M. Smith and H. W. Peter Beadle, "Smartbadges: A wearable computer and communication system," *Proc. of the 6<sup>th</sup> International Workshop on Hardware/Software Codesign*, Invited Talk, Mar. 1998.
- [9] L. Naimark and E. Foxlin, "Circular Data Matrix Fiducial System and Robust Image Processing for a Wearable Vision-Inertial Self-tracker," *Proc. of the 1<sup>st</sup> IEEE and ACM International Symposium on Mixed and Augmented Reality (ISMAR02)*, pp. 27-36, Sep. 2002.
- [10] W. Piekarski and B. H. Thomas, "The Tinmith System - Demonstrating New Techniques for Mobile Augmented Reality Modeling," *Proc. of the 3<sup>rd</sup> Australasian User Interfaces Conference*, pp. 61-70, Jan. 2002.
- [11] M. Ribo, P. Lang, H. Ganster, M. Brandner, C. Stock, and A. Pinz "Hybrid Tracking for Outdoor Augmented Reality Applications," *IEEE Computer Graphics and Applications*, Vol. 22, No. 6, pp. 54-63, Nov./Dec. 2002.
- [12] R. Tenmoku, M. Kanbara and N. Yokoya, "A Wearable Augmented Reality System Using Positioning Infrastructures and a Pedometer," *Proc. of the 7<sup>th</sup> IEEE International Symposium on Wearable Computers (ISWC03)*, pp. 110-117, Oct. 2003.
- [13] G. Welch and G. Bishop, "SCAAT: Incremental Tracking with Incomplete Information," *Proc. of ACM SIGGRAPH '97*, pp. 333-344, Aug. 1997.
- [14] G. Welch and E. Foxlin, "Motion Tracking: No Silver Bullet, but a Respectable Arsenal," *IEEE Computer Graphics and Applications*, Vol. 22, No. 6, pp. 24-38, Nov./Dec. 2002.